Application of Cascade Nonlinear Control for a CSTR

PETR DOSTÁL, VLADIMÍR BOBÁL, and JIŘÍ VOJTĚŠEK
Faculty of Applied Informatics, Tomas Bata University in Zlin,
Nad Stranemi 4511, 760 05 Zlin, Czech Republic
{dostalp;bobal;vojtesek}@fai.utb.cz http://www.fai.utb.cz/

Abstract: —The article deals with the cascade nonlinear control of a chemical continuous stirred tank reactor. The control is performed in primary and secondary control-loops where the primary controlled output of the reactor is a concentration of the main reaction product and the secondary output is the reactant temperature. A common control input is the coolant flow rate. The controller in the primary control-loop is a P-controller with an adjustable gain. A controller in the secondary control-loop consist of the static nonlinear and the dynamic adaptive linear part. The proposed method is verified by control simulations.

Keywords: —chemical reactor, cascade control, nonlinear control, external linear model, adaptive control.

1 Introduction

The cascade control belongs to more complex control structures useful for such processes where more output variables can be measured and where only one input variable is available to the control. Principles of the cascade control are described e.g. in [1], [2] and [3].

Chemical reactors are typical processes suitable for a use of the cascade control. In cases of non-isothermal reactions, concentrations of the reaction products mostly depend on the temperature of reactant. Further, it is known that while the reactant temperature can be measured almost continuously, see, e.g. [4], concentrations are usually measured in longer time intervals. Then, the application of the cascade control method can lead to good results. In this paper, the procedure for the cascade control design of a continuous stirred tank chemical reactor is presented.

Continuous stirred tank reactors (CSTRs) are units frequently used in chemical industry. From the system theory point of view, CSTRs belong to the class of nonlinear systems. Their mathematical models are described by sets of nonlinear differential equations (ODEs). The methods of CSTRs modelling and simulation can be found e.g. in [5] and [6].

In this paper, the CSTR control strategy is based on the fact that concentrations of components of reactions taking place in the reactor depend on the reactant temperature. Then, the main product concentration is considered as the primary controlled variable, and, the reactant temperature as the secondary controlled variable. The coolant flow rate represents a common control input. The primary controller determining the set point for the secondary (inner) control-loop is a P-controller with an adjustable gain. For the secondary controller, the procedure based on its factorization on linear and nonlinear parts is used. Basic ideas of this method can be found e.g. in [7] – [9]. The nonlinear static part (NSP) is obtained from simulated or measured steady-state characteristic of the CSTR, its polynomial or exponential approximation, and, subsequently, its differentiation. On behalf of development of the linear dynamic part (LDP), the NSP including the nonlinear model of the CSTR is approximated by a CT external linear model (ELM). For the CT ELM parameter estimation, the direct estimation in terms of filtered variables is used, see e.g. [10] – [13]. The method is based on filtration of continuous-time input and output signals where the filtered variables have in the s-domain the same properties as their non-filtered counterparts. The resulting CT controller is derived on the basis of the pole placement method, see, e.g. [14] – [17]. Some other procedures and methods related to the issue are described e.g. in [19] – [23]. The control is tested by simulations of nonlinear model of the CSTR with a consecutive exothermic reaction.

2 Model of the CSTR

Consider a CSTR with the first order consecutive exothermic reaction according to the scheme $A \xrightarrow{k_1} B \xrightarrow{k_2} C$ and with a perfectly mixed cooling jacket. Using the usual simplifications, the model of the CSTR is described by four nonlinear differential equations

$$\frac{dc_A}{dt} = -\left(\frac{q_r}{V_r} + k_1\right)c_A + \frac{q_r}{V_r}c_{Af} \qquad (1)$$

$$\frac{dc_B}{dt} = -\left(\frac{q_r}{V_r} + k_2\right)c_B + k_1 c_A + \frac{q_r}{V_r}c_{Bf} \quad (2)$$

$$\frac{dT_r}{dt} = \frac{h_r}{(\rho c_p)_r} + \frac{q_r}{V_r}(T_{rf} - T_r) + \frac{A_h U}{V_r(\rho c_p)_r}(T_c - T_r) \quad (3)$$

$$\frac{dT_c}{dt} = \frac{q_c}{V_c}(T_{cf} - T_c) + \frac{A_h U}{V_c(\rho c_p)_c}(T_r - T_c) \quad (4)$$

with initial conditions $c_A(0) = c_A^s$, $c_B(0) = c_B^s$, $T_r(0) = T_r^s$ and $T_c(0) = T_c^s$. Here, t stands for the time, c for concentrations, T for temperatures, V for volumes, ρ for densities, c_p for specific heat capacities, q for volumetric flow rates, A_h is the heat exchange surface area and U is the heat transfer coefficient. Subscripts denoted r describe the reactant mixture, c the coolant, f the inlet values and the superscript s steady-state values.

The reaction rates and the reaction heat are expressed as

$$k_j = k_{0j}\exp\left(\frac{-E_j}{RT_r}\right),\ j = 1,2 \quad (5)$$

$$h_r = h_1 k_1 c_A + h_2 k_2 c_B \quad (6)$$

where k_0 are pre-exponential factors, E are activation energies and h are reaction enthalpies. The values of parameters, feed values and steady-state values are given in Table 1.

Table 1: Parameters and inlet values

V_r = 1.2 m^3 V_c = 0.64 m^3 ρ_r = 985 kg m^{-3} ρ_c = 998 kg m^{-3}	c_{pr} = 4.05 kJ kg^{-1}K^{-1} c_{pc} = 4.18 kJ kg^{-1}K^{-1} A_h = 5.5 m^2 U = 43.5 kJ m^{-2}min^{-1}K^{-1}
k_{10} = 5.616 · 10^{16} min^{-1} k_{20} = 1.128 · 10^{18} min^{-1} h_1 = 4.8 · 10^4 kJ kmol^{-1}	E_1/R = 13477 K E_2/R = 15290 K h_2 = 2.2 · 10^4 kJ kmol^{-1}
c_{Af}^s = 2.85 kmol m^{-3} T_{rf}^s = 323 K	c_{Bf}^s = 0 kmol m^{-3} T_{cf}^s = 293 K
q_r^s = 0.08 m^{3}min^{-1}	

The desired reaction product is a concentration of the component B.

3 Control System Design

A basic scheme of the cascade control is in Fig. 1.

Here, PC stands for the primary proportional controller, LDP for the linear part and NSP for the

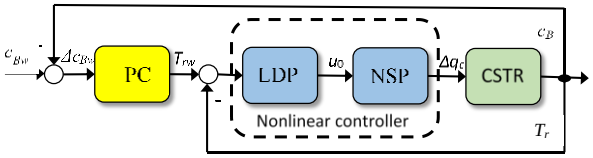

Fig. 1: Cascade nonlinear control scheme.

nonlinear part of the secondary controller and CSTR for the reactor.

The control objective is to achieve a concentration of the component B as the primary controlled output near to its maximum. A dependence of the concentration c_B on the reactant temperature is in Fig. 2.

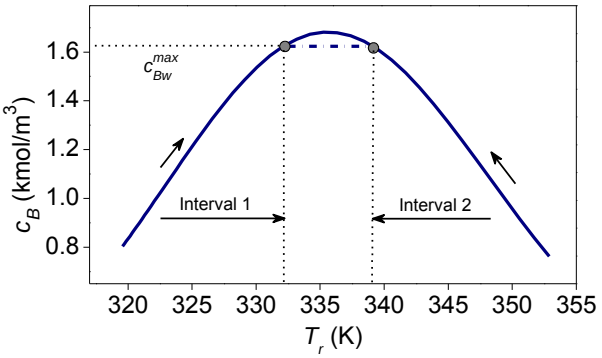

Fig. 2: Steady-state dependence of the product B concentration on the reactant temperature.

There, an operating area consists of two intervals. In the first interval, the concentration B increases with increasing reactant temperature, in the second interval it again decreases. Both intervals are limited by the maximum value $c_B^{\max}$ = 1.62 kmol/m2. It can be seen that the maximum value of c_B can be slightly higher then $c_B^{\max}$. However, with respect to some following procedures, the maximum desired value of c_B will be limited just by $c_B^{\max}$.

4 Primary Controller Design

The primary P-controller controller realizes the relation between the deviation of desired and actual concentration c_B and the corresponding desired reaction temperature according to the equation

$$\Delta T_{rw} = G_w \Delta c_{Bw} \quad (7)$$

where G_w is an adjustable gain.

5 Secondary Controller Desig

As previously introduced, the secondary controller

consist of a nonlinear static and an adaptive linear dynamic part. The LDP creates a linear dynamic relation $u_0(t) = \Delta T_w(t)$ which represents a difference of the reactant temperature adequate to its desired value. Then, the NSP generates a static nonlinear relation betveen u_0 and a corresponding increment (decrement) of the coolant flow rate.

5.1 Nonlinear Static Part

The NSP derivation appears from a simulated or measured steady-state characteristics. The dependence of the reactant temperature on the coolant flow rate is shown in Fig.3. Both intervals are in accordance with intervals in Fig.2.

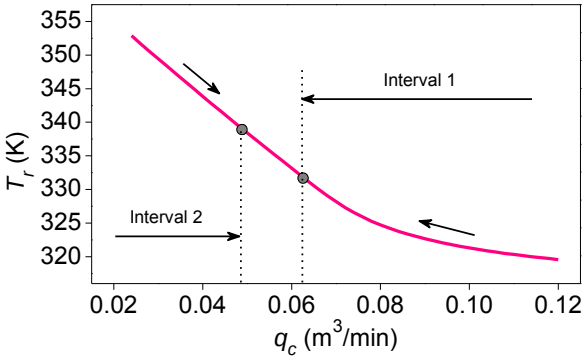

Fig. 3: Dependence of the reactant temperature on the coolant flow rate in the steady-state.

For purposes of later procedures, the boundaries of both intervals are determined as

$$0.12 \geq q_c \geq 0.062\,,\ 319.58 \leq T_r \leq 332.12$$

in the first operating interval, and,

$$0.049 \geq q_c \geq 0.024\,,\ 339.1 \leq T_r \leq 352.9$$

in the second operating interval.
With respect to required approximations, both coordinates are transformed as

$$\theta = \frac{q_c - q_c^{\min}}{q_c^{\max} - q_c^{\min}}\ ,\quad \theta \in <0,1> \tag{8}$$

$$\psi = \frac{T_r - T_r^{\min}}{T_r^{\max} - T_r^{\min}}\ ,\quad \psi \in <0,1> \tag{9}$$

where

$q_c^{\min} = 0.024$, $q_c^{\max} = 0.12$, $T_r^{\min} = 319.58$,
$T_r^{\max} = 352.9$.

Then, transformed characteristics in both intervals are approximated as

$$\psi = -0.028 + 2.1336 \exp(-\theta / 0.2383) \tag{10}$$

In the first interval, and,

$$\psi = 0.9965 - 1.6017\,\theta \tag{11}$$

in the second interval. The characteristics in both intervals together with their approximations are shown in Figs.4 and 5.

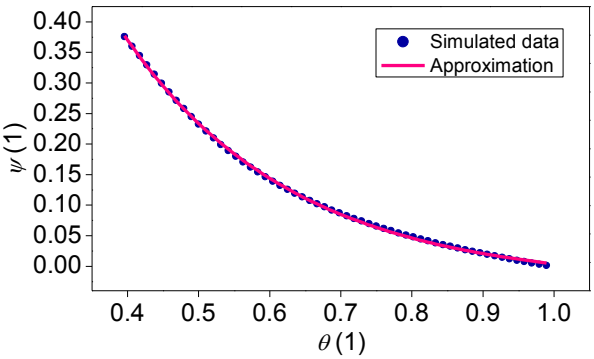

Fig. 4: Transformed steady state-characteristics in interval 1with approximation.

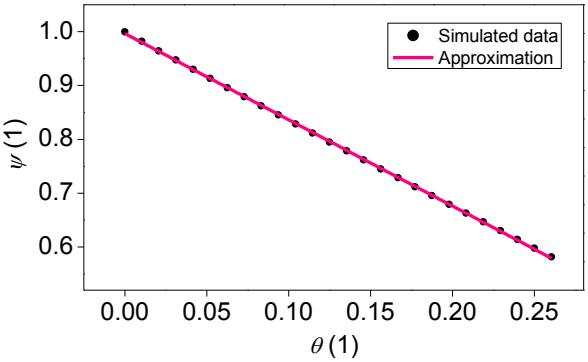

Fig. 5: Transformed steady state-characteristics in interval 2 with approximation.

Derivatives of expressions (10) and (11) needed to determine the function of the NSP are

$$\frac{d\psi}{d\theta} = -8.9534 \exp(-\frac{\theta}{0.2383}) \tag{12}$$

in the first interval, and,

$$\frac{d\psi}{d\theta} = -1.6017 \tag{13}$$

in the second interval.
The relation between input and output of the NPC can now be formulated as

$$\Delta q_c = \frac{q_c^{\max} - q_c^{\min}}{T_r^{\max} - T_r^{\min}} \left(1 / \frac{d\psi}{d\theta}\right)_{\psi(T_r)} u_0 \tag{14}$$

where u_0 is the output of the LDP and $\psi(T_r)$ je a value of ψ according to T_r on the output of the CSTR.

5.2 CT External Linear Model

The nonlinear component of the closed-loop consisting of the NSP of the controller and the CSTR nonlinear model is approximated by a continuous-time external linear model (CT ELM) according to Fig. 6.

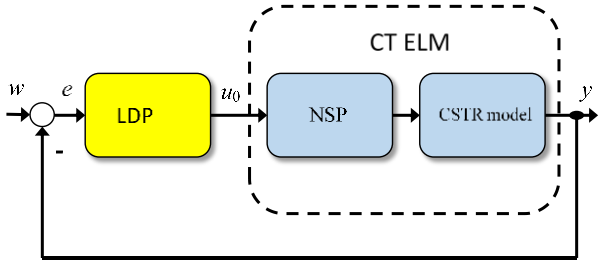

Fig. 6: Control system with CT external linear model.

where $w = \Delta T_{rw}$ and $y = T_r - T_r^s$.

It is well known that in adaptive control the controlled process of a higher order can be approximated by a linear model of a lower order with varying parameters. Here, the second order CT ELM has been chosen in the form of the second order linear differential equation

$$\ddot{y}(t) + a_1 \dot{y}(t) + a_0 y(t) = b_0 u_0(t) \tag{15}$$

and, in the complex domain, as the transfer function

$$G(s) = \frac{Y(s)}{U_0(s)} = \frac{b_0}{s^2 + a_1 s + a_0} \tag{16}$$

5.3 CT ELM Parameter Estimation

The method of the direct CT ELM parameter estimation can be briefly carried out as follows.

Since the derivatives of both input and output cannot be directly measured, filtered variables u_f and y_f are established as the outputs of filters

$$c(\sigma) u_f(t) = u(t) \tag{17}$$

$$c(\sigma) y_f(t) = y(t) \tag{18}$$

where $\sigma = d/dt$ is the derivative operator, $c(\sigma)$ is a stable polynomial in σ that fulfills the condition $\deg c(\sigma) \geq \deg a(\sigma)$.

Note that the time constants of filters must be smaller than the time constants of the process. Since the latter are unknown at the beginning of the estimation procedure, it is necessary to make the filter time constants, selected a priori, sufficiently small.

With regard to (16), the polynomial a takes the concrete form $a(\sigma) = \sigma^2 + a_1 \sigma + a_0$, and, the polynomial c can be chosen as $c(\sigma) = \sigma^2 + c_1 \sigma + c_0$. Subsequently, the values of the filtered variables can be computed during the control by a solution of (17) and (18) using some standard integration method.

It can be easily proved that the transfer behavior among filtered and among nonfiltered variables are equivalent. Using the L-transform of (17) and (18), the expressions

$$c(s) U_f(s) = U(s) + \mu_1(s) \tag{19}$$

$$c(s) Y_f(s) = Y(s) + \mu_2(s) \tag{20}$$

can be obtained with μ_1 and μ_2 as polynomials of initial conditions. Substituting (19) and (20) into (16), and, after some manipulations, the relation between transforms of the filtered input and output takes the form

$$\begin{aligned} Y_f(s) &= \frac{b(s)}{a(s)} U_f(s) + M(s) = \\ &= G(s) U_f(s) + M(s) \end{aligned} \tag{21}$$

where $M(s)$ is a rational function as the transform of any function $\mu(t)$ which expresses an influence of initial conditions of filtered variables.

Now, the filtered variables including their derivatives can be sampled from filters (19) and (20) in discrete time intervals $t_k = k\, T_S$, $k = 0,1,2, \ldots$ where T_S is the sampling period. Denoting deg $a = n$ and deg $b = m$, the regression vector is defined as

$$\begin{aligned} \boldsymbol{\Phi}(t_k) = \big[& -y_f(t_k) - y_f^{(1)}(t_k) \ldots - y_f^{(n-1)}(t_k) \\ & u_f(t_k)\, u_f^{(1)}(t_k) \ldots u_f^{(m)}(t_k)\ 1 \big] \end{aligned} \tag{22}$$

Then, the vector of parameters

$$\boldsymbol{\Theta}^T(t_k) = \left[a_0\ a_1 \ldots a_{n-1}\ b_0\ b_1 \ldots b_m \right] \tag{23}$$

can be estimated from the ARX model

$$y_f^{(n)}(t_k) = \boldsymbol{\Theta}^T(t_k) \Phi(t_k) + \mu(t_k) \tag{24}$$

Here, the recursive identification method with exponential and directional forgetting was used according to [18].

5.4 Linear Dynamic Part

For the adaptive control purposes, the 2DOF controller is used. It is known that this type of the controller often provides smoother control actions then a standard feedback controller. The 2DOF controller consist of the feedback part Q and the feedforward part R as shown in Fig. 7.

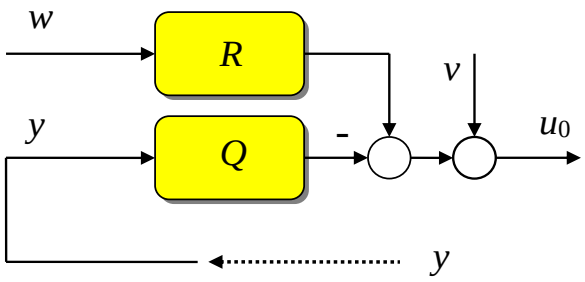

Fig. 7: The 2DOF controller.

In the scheme, w is the reference signal, y is the controlled output and u_0 the controller output. The reference w is taken into account as a sequence of step functions with transforms

$$W_k(s) = \frac{w_{k0}}{s} \tag{25}$$

In this paper, a disturbance is not considered.
The transfer functions of both controller parts are in forms

$$R(s) = \frac{r(s)}{p(s)}, \quad Q(s) = \frac{q(s)}{p(s)} \tag{26}$$

where q, r and p are coprime polynomials in s fulfilling the condition of properness $\deg r \le \deg p$ and $\deg q \le \deg p$. For a step disturbance with the transform (28), the polynomial p takes the form $p(s) = s\,\tilde{p}(s)$.
Using the polynomial theory, the controller results from a couple of polynomial equations

$$a(s)s\,\tilde{p}(s) + b(s)q(s) = d(s) \tag{27}$$

$$t(s)s + b(s)r(s) = d(s) \tag{28}$$

with a stable polynomial d on their right sides.
For the transfer function (16) with deg a = 2, the controller transfer functions take forms

$$Q(s) = \frac{q(s)}{s\,\tilde{p}(s)} = \frac{q_2 s^2 + q_1 s + q_0}{s(s + p_0)}$$
$$R(s) = \frac{r(s)}{s\,\tilde{p}(s)} = \frac{r_0}{s(s + p_0)} \tag{29}$$

Moreover, the equality $r_0 = q_0$ can easily be obtained.
The controller parameters then follow from solutions of polynomial equations (27) and (28) and depend upon coefficients of the polynomial d.
In this paper, the polynomial d with roots determining the closed-loop poles is chosen as

$$d(s) = n(s)(s + \alpha)^2 \tag{30}$$

where n is a stable polynomial obtained by spectral factorization

$$a^*(s)a(s) = n^*(s)n(s) \tag{31}$$

and α is the selectable parameter that can usually be chosen by way of simulation experiments. Note that a choice of d in the form (30) provides the control of a good quality for aperiodic controlled processes. The polynomial n has the form

$$n(s) = s^2 + n_1 s + n_0 \tag{32}$$

with coefficients

$$n_0 = \sqrt{a_0^2}, \quad n_1 = \sqrt{a_1^2 + 2n_0 - 2a_0}. \tag{33}$$

The controller parameters can be obtained from solution of the matrix equation

$$\begin{pmatrix} 1 & 0 & 0 & 0 \\ a_1 & b_0 & 0 & 0 \\ a_0 & 0 & b_0 & 0 \\ 0 & 0 & 0 & b_0 \end{pmatrix} \begin{pmatrix} p_0 \\ q_2 \\ q_1 \\ q_0 \end{pmatrix} = \begin{pmatrix} d_3 - a_1 \\ d_2 - a_0 \\ d_1 \\ d_0 \end{pmatrix} \tag{34}$$

where

$$d_3 = n_1 + 2\alpha,\ d_2 = 2\alpha n_1 + n_0 + \alpha^2$$
$$d_1 = 2\alpha n_0 + \alpha^2 n_1,\ d_0 = \alpha^2 n_0 \tag{35}$$

Evidently, the controller parameters can be adjusted by the selectable parameter α.

6 Simulation Results

All simulations were performed on nonlinear model of the CSTR. Considering the measurement of the concentration c_B in periods τ_s (min), the aim of simulations is to show an effect of this period and an effect of the adjustable gain of the P-controller G_w on some control responses. At the start of simulations, the P controller with a small gain was used. For the direct recursive parameter estimation, the sampling period T_S = 1 min was chosen. The value of the selectable parameter α is stated under each figure.
In the first case, simulations in the first operating interval were performed. Here, all simulations started from the point $c_B^s = 1.2$ kmol/m^3 and $q_c^s = 0.08$ m^3/min. The desired value of c_B has been chosen as $c_{Bw} = 1.6$ kmol/m^3 Effect of the parameter G_w on the reference w, the reactant temperature T_r and the concentration c_B responses is evident from Figs. 8, 9 and 10.

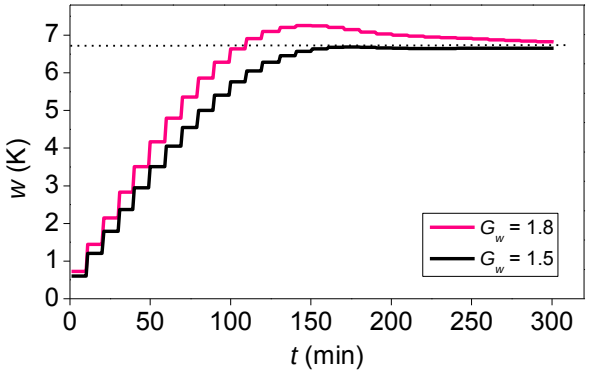

Fig. 8: Reference signal courses (τ_s = 10, α = 0.2).

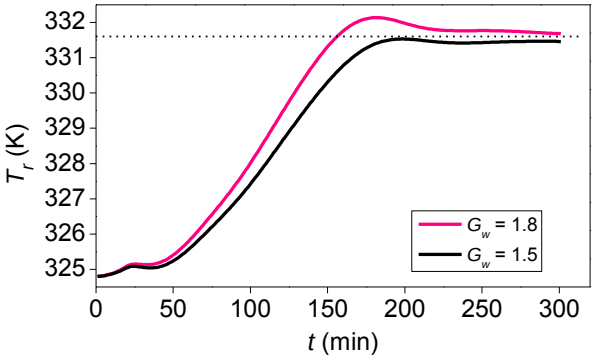

Fig. 9: Reactant temperature responses (τ_s = 10, α = 0.2).

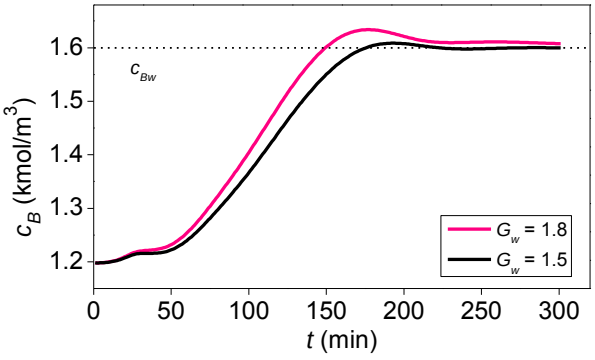

Fig. 10: Concentration c_B responses (τ_s = 10, α = 0.2).

It can be seen that an increasing G_w accelerates both signals in the control loop. However, its value is not unrestricted and its convenient value should be found experimentally. Strong sensitivity of the period τs on all responses can be seen in Figs.11, 12 and 13. Its shortening leads to significant overshoots. These, however, can be suppressed by setting a lower gain G_w. It should be to realize that τs is determined by possibilities of measurement.

Of interest, the coolant flow courses during control and under the same conditions can be seen in Fig. 14.

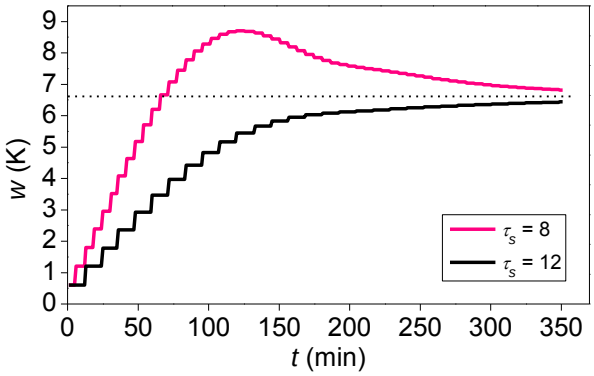

Fig. 11: Reference signal courses (G_w = 1.5, α = 0.2).

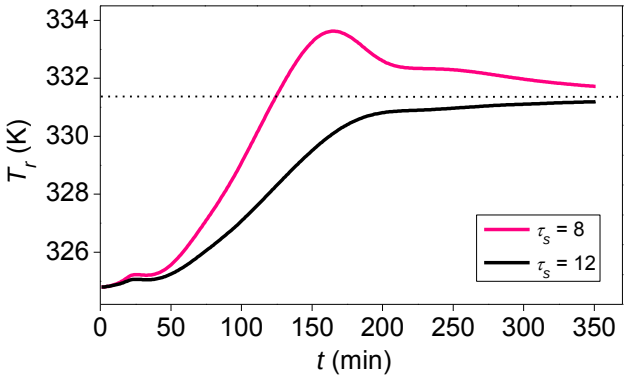

Fig. 12: Reactant temperature responses (G_w = 1.5, α = 0.2).

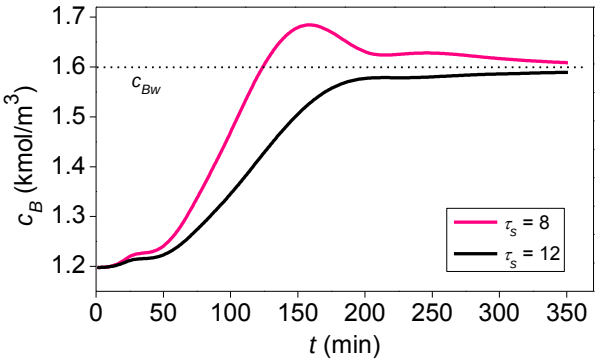

Fig. 13: Concentration c_B responses (G_w = 1.5, α = 0.2).

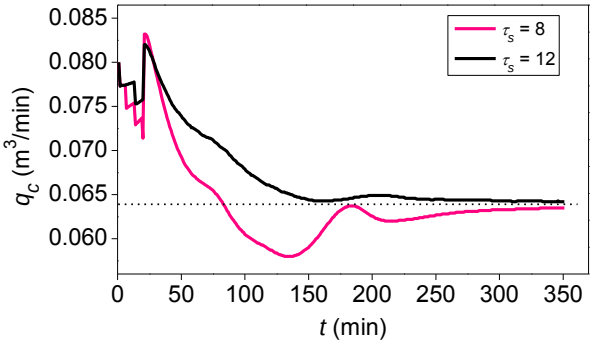

Fig. 14: Coolant flow rate courses (G_w = 1.5, α = 0.2).

Next simulations were performed in the interval 2. Here, all simulations started from the point $c_B^s = 0.917\ \text{kmol/m}^3$ and $q_c^s = 0.028\ \text{m}^3/\text{min}$. An effect of selectable parameters G_w and t_s is similar as in the first interval.

The adaptive controller parameters depend upon the selection of the parameter α. An effect of this parameter is not very significant and it can be seen in Figs. 23 and 24.

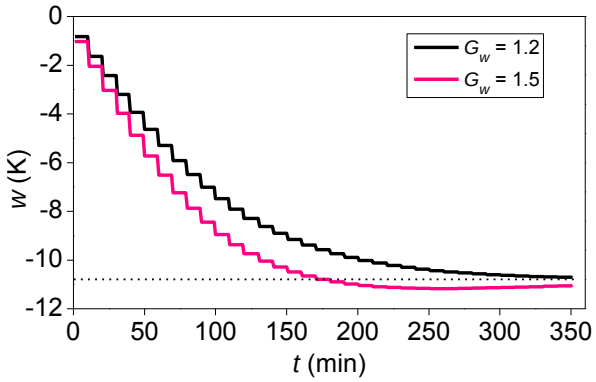

Fig. 15: Reference signal courses (τ_s = 10, α = 0.1).

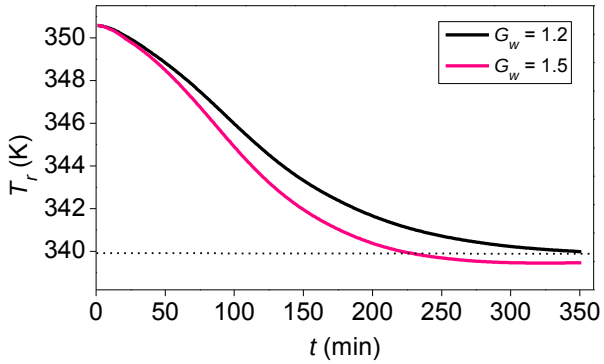

Fig. 16: Reactant temperature responses (τ_s = 10, α = 0.1).

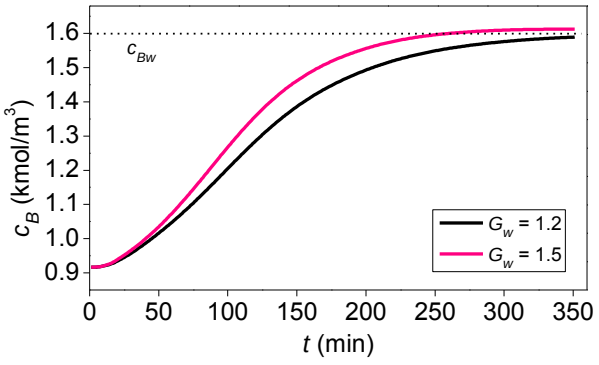

Fig. 17: Concentration c_B responses (τ_s = 10, α = 0.1).

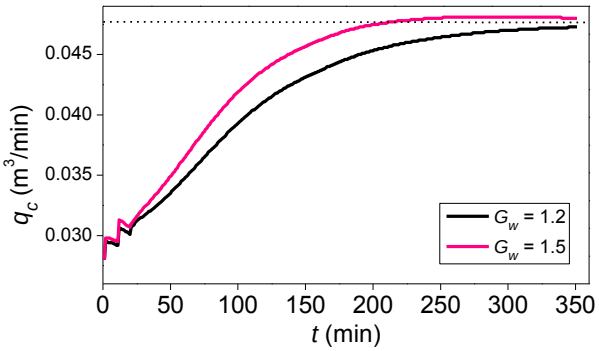

Fig. 18: Coolant flow rate courses (t_s = 1.5, α = 0.1).

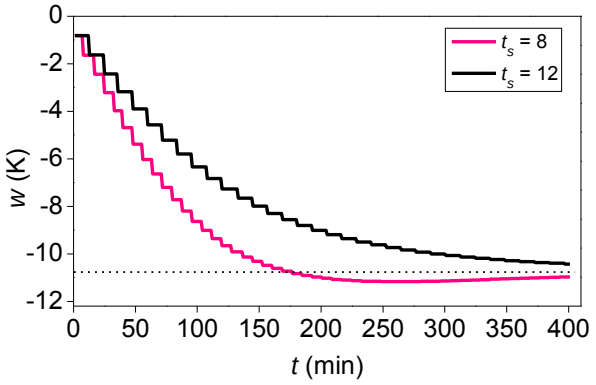

Fig. 19: Reference signal courses (G_w = 1.2, α = 0.1).

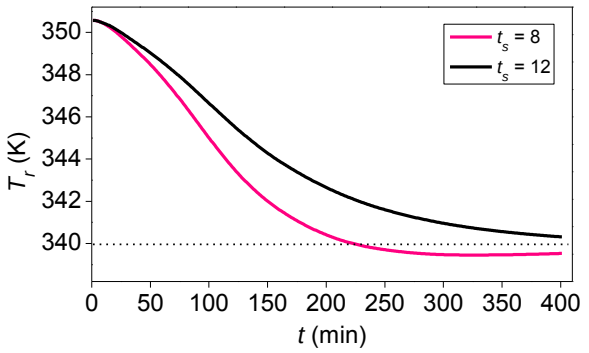

Fig. 20: Reactant temperature responses (G_w = 1.2, α = 0.1).

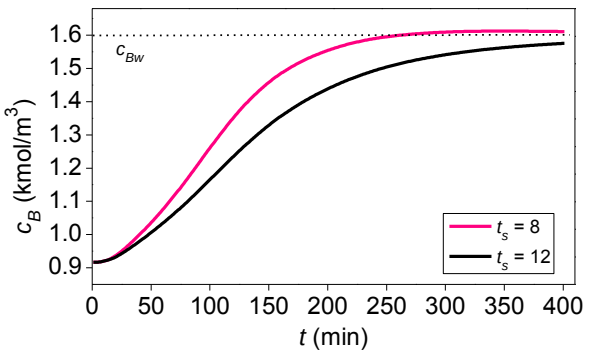

Fig. 21: Concentration c_B responses (G_w = 1.2, α = 0.1).

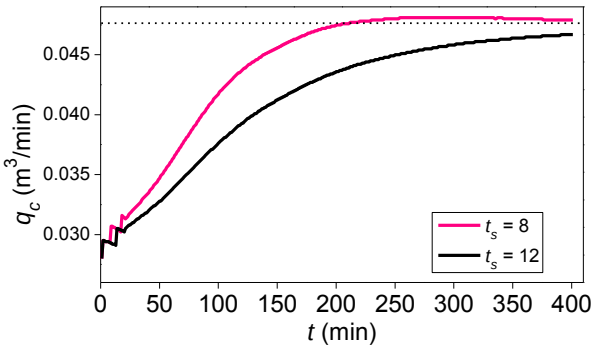

Fig. 22: Coolant flow rate courses (t_s = 1.5, α = 0.1).

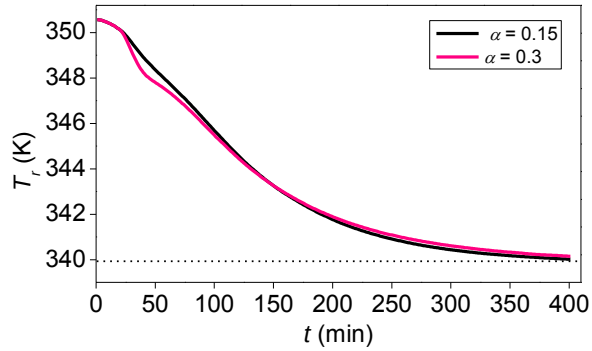

Fig. 23: Reactant temperature responses (G_w = 1.2, t_s = 10).

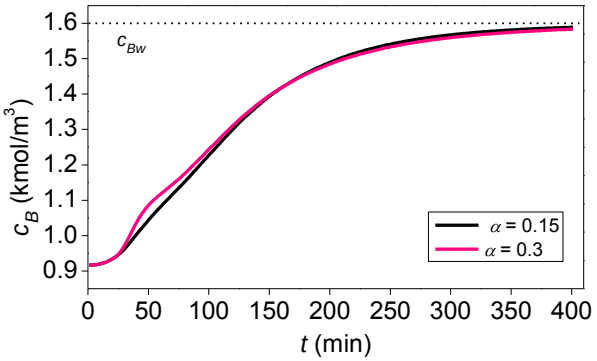

Fig. 24: Concentration c_B responses (G_w = 1.2, t_s = 10).

7 Conclusions

The paper deals with the cascade nonlinear control of a continuous stirred tank reactor. The control is performed in the external (primary) and inner (secondary) closed-loop where the concentration of a main product is the primary and the reactant temperature the secondary controlled variable. A common control input is the coolant flow rate.

The controller in the external control-loop is a P-controller with an adjustable gain. The controller in the inner control-loop is a nonlinear controller consisting of a nonlinear static part and an adaptive linear dynamic part in the 2DOF structure. For its derivation, the recursive parameter estimation, the polynomial approach and the pole placement method were applied.

The control was tested by simulations on the nonlinear model of the CSTR.

References

[1] J. F. Smuts, *Process Control for Practitioners*, OptiControls Inc., New York, 2011.

[2] M. King, *Process Control: A Practical Approach*, John Wiley & Sons, Chichester, 2010.

[3] D.E. Seborg, T.F. Edgar, and D.A. Mellichamp, *Process Dynamics and Control*, John Wiley and Sons, Chichester, 1989.

[4] Jiu-Qiang Zhao, Xiao-Fen Li, Zhi Cheng, and Guang Chen, A linear temperature measurement system based on Cu100, *WSEAS Transactions on Systems*, Vol. 13, 2014, pp. 648-659.

[5] J.-P. Corriou, *Process control. Theory and applications*, Springer – Verlag, London, 2004.

[6] J. Ingham, I.J. Dunn, E. Heinzle, and J.E. Přenosil, *Chemical Engineering Dynamics. Modelling with PC Simulation*, VCH Verlagsgesellschaft, Weinheim, 1994..

[7] Cs. Bányász, and L. Keviczky, L., A simple PID regulator applicable for a class of factorable nonlinear plants, in *Proc. American Control Conference*, Anchorage, Alaska, 2002, pp. 2354-2359.

[8] Chyi-Tsong Chen1, Yao-Chen Chuang1, and Yao-Chen Hwang, A simple nonlinear control strategy for chemical processes, in *Proc. 6th Asian Control Conference*, Bali, Indonesia, 2006, pp. 64-70.

[9] J. Vörös, Recursive identification of Wiener systems with two segment polynomial nonlinearities, *Journal of Electrical Engineering*, Vol. 59(1), 2008, pp. 40-44.

[10] P. Dostál, V. Bobál, J. Vojtěšek, and B. Chramcov, Adaptive control of nonlinear processes using two methods of parameter estimation, *WSEAS Transactions on Systems*, 2014, Vol. 13, 2014, pp. 292-301.

[11] G.P. Rao, and H. Unbehauen, Identification of continuous-time systems, *IEE Proc.-Control Theory Appl.*, Vol. 153, 2006, pp. 185-220.

[12] H. Garnier, and L. Wang (eds.), *Identification of continuous-time models from sampled data*, Springer-Verlag, London, 2008.

[13] P. Dostál, V. Bobál, and F. Gazdoš, Adaptive control of nonlinear processes: Continuous-time versus delta model parameter estimation, in *IFAC Workshop on Adaptation and Learning in Control and Signal Processing ALCOSP 04*, Yokohama, Japan, 2004, pp. 273-278.

[14] M.J. Grimble, *Robust industrial control. Optimal design approach for polynomial systems*, Prentice Hall, London, 1994.

[15] V. Kučera, Diophantine equations in control – A survey, *Automatica*, Vol. 29, 1993, pp. 1361-1375.

[16] P. Dostál, J. Vojtěšek, and V. Bobál, Adaptive LQ control of a shell and tube heat exchanger, *International Journal of Mathematics and Computers in Simulations*, Vol. 7, 2013, pp. 389-397.

[17] P. Dostál, J. Vojtěšek, and V. Bobál, Simulation of adaptive temperature control in a tubular chemical reactor, *International Review on Modelling and Simulations*, 2012, Vol. 5, pp. 1049-1058.

[18] V. Bobál, J. Böhm, J. Fessl, and J. Macháček, *Digital self-tuning controllers*, Springer Verlag, Berlin, 2005.

[19] S. Staines, and F. Neri, A matrix transition oriented net for modeling distributed complex computer and communication systems, *WSEAS Transactions on Systems*, Vol. 13, 2014, pp. 12-22.

[20] M. Camilleri, F. Neri, and M. Papoutsidakis, An algorithmic approach to parameter selection in machine learning using Meta-Optimization techniques, *WSEAS Transactions on Systems*, Vol. 13, 2014, pp. 202-213.

[21] M. Papoutsidakis, D. Piromalis, F. Neri, and M. Camilleri, Intelligent algorithms based on data processing for modular robotic vehicles control, *WSEAS Transactions on Systems*, Vol. 13, 2014, 242-251.

[22] E. Gyurkovics, and T. Takacs, LMI based bounded output feedback control for uncertain systems, *WSEAS Transactions on Systems*, Vol. 13, 2014, pp. 679-689.

[23] V. Bobál, M. Kubalčík, P. Dostál, J. Novák, Adaptive predictive control of laboratory heat exchanger, *WSEAS Transactions on Systems*, Vol. 13, 2014, pp. 470-481.